Electron tunneling spectroscopy of single-crystal $Bi_2Sr_2CaCu_2O_8$

H. J. Tao,* A. Chang, Farun Lu, and E. L. Wolf
Polytechnic University, Brooklyn, New York 11201
(Received 3 September 1991; revised manuscript received 26 November 1991)

The T-dependent conductance $G(V,T)$ of evaporated Pb junctions on cleaved ab planes of $Bi_2Sr_2CaCu_2O_8$ (2:2:1:2) crystals is presented. Strong superconducting $G_s(V,T)$ structures imply a large gap, approximately $\Delta_0(0)=26$ meV, or $2\Delta_0(0)/k_BT_c=6.7$. An analysis of $G(V,T)$ near T_c, assuming a lifetime-broadened BCS $N_s(E)$, reveals a broadening $\Gamma(T)$ such that $\Delta(T_c)\approx\Gamma(T_c)\approx 2k_BT_c$. The fitted $\Delta(T_c)$, unlike typical BCS values, is $\approx 0.8\Delta(0)$. $G(V, T>T_c)$ has a minimum at $V=0$, suggestive of known c-direction localization in 2:2:1:2 compounds. $G(V,T)$ also reveals the expected fluctuation superconductivity above T_c. 4.2-K scanning-tunneling-microscope (STM) spectra are mentioned in comparison. A larger gap, about 40 meV, and dip at 80 meV, found in the STM $G(V)$ are tentatively attributed to CuO_2 planes.

I. INTRODUCTION

Tunneling spectroscopy provides a detailed probe of the superconducting state with accurate values of gap edges and precise measurements of density of states (DOS) of quasiparticles.[1,2] Measurement of the normalized tunneling conductance

$$\frac{(dI/dV)_s}{(dI/dV)_n}=\frac{G_s(V,T)}{G_n(V)} ,$$

of a normal-metal–insulator–superconductor (N-I-S) junction measures the energy spectrum of excitations, $N_s(E)$, with resolution about $3.5k_BT$. Thus

$$G_s(V)=-\int_{-\infty}^{\infty}|M|^2\rho_n(E)N_s(E)\frac{d[f(E-V)]}{d(eV)} , \quad (1)$$

where $\rho_n(E)$ is the normal density of states, M the tunneling matrix element, and $f=[1+\exp(eV/k_BT)]^{-1}$. The convolution of $N_s(E)$ with $-df/d(eV)$, to describe partial occupation of states near the normal metal E_F, broadens the structure in $N_s(E)$ to a full width at half maximum (FWHM) of $3.5k_BT$. At $T=0$, or if $\Gamma\gg k_BT$, as may occur in a gapless superconductor, one obtains $G_s/G_n\approx N_s(V)$.

Conventional superconductors can be made gapless by the addition of magnetic impurities, e.g., Pb:Mn. In spin-exchange collisions with magnetic impurities, singlet pairs are broken at the rate Γ. A level broadening Γ which is large near T_c and falls sharply below T_c appears to be a fundamental aspect of high-T_c superconductivity.[3] A convenient and intuitive $N_s(E)$ (Ref. 4) to treat lifetime energy broadening is a BCS function with $i\Gamma=i\hbar/\tau$ added to the energy E:

$$N_{\text{Dynes}}(E)=\text{Re}\{(E+i\Gamma)^2/[(E+i\Gamma)^2-\Delta^2]\}^{1/2} . \quad (2)$$

$N_{\text{Dynes}}(E)$ is an interpolation function for the $N_s(E)$ produced by spin fluctuations[4] and, for lack of a better function, is often used in fitting high-T_c tunneling data. It is most appropriate near T_c where level broadening is important.

We find that $N_{\text{Dynes}}(E)$ is quantitatively useful in fitting the measured $G_s(V)$ near T_c, where $N_s(E)$ is strongly affected by the lifetime broadening, although it does not accurately fit for $T\ll T_c$. In this paper the normalized conductance obtained by substituting (2) in (1) is designated $G_{\text{Dynes}}(V,\Delta,\Gamma,T)$, where V, Δ, Γ, and T, respectively, are bias voltage, energy gap, energy broadening (all in meV), and temperature in kelvins. (In connection with the figures D,G are used for Δ,Γ.) We emphasize that all fits here include thermal broadening via Eq. (1).

The use of Eq. (2), even though we find that it does not accurately fit the ground state, deserves some comment. First, Eq. (2) does fit the data in the range near T_c, where level broadening is important, from which one may expect physically meaningful derived parameters. Second, on a more fundamental level, one may find near T_c in systems with appreciable level broadening something approaching universal behavior. A general function applicable near T_c is given[5] by de Gennes: $N(E)=1+(\Delta^2/2)(E^2-\Gamma^2)/(E^2+\Gamma^2)$. We verified that the expansion of Eq. (2) is identical to this when $\Gamma^2+E^2\gg\Delta^2$, i.e., for systems with strong broadening near T_c. Thus we expect Eq. (2) to be rather widely applicable near T_c when level broadening is present. These considerations justify using Eq. (2) and allow us to attach physical meaning to the derived parameters Δ and Γ in the region near T_c, even though the function accurately describing the ground state, $N_s(E, T=0)$, is not known.

Considerable effort has been expended on tunneling investigation of high-T_c superconductors. For cubic $Ba_{1-x}K_xBiO_3$, a BCS density of states with $2\Delta/k_BT_c=3.8$–3.9, $\alpha^2F(\omega)$, and other microscopic parameters have recently been obtained by Huang *et al.*[6] Tunneling results on films of the least anisotropic cuprate, $YBa_2Cu_3O_{7-x}$ (Y-Ba-Cu-O), have been reported[7] and on etched crystals by Gurvitch *et al.*[8] $Bi_2Sr_2CaCu_2O_8$ (2:2:1:2) does not have the Cu-O chains of Y-Ba-Cu-O and thus is a more basic cuprate. The 2:2:1:2 structure also exhibits a greater anisotropy in resistivity ρ and coherence length ξ than Y-Ba-Cu-O. The resistivity in the c direction, ρ_c, is nonmetallic in nature, with

$\rho_c/\rho_{ab} \sim 10^5$.[9] Tunneling into Bi-Sr-Ca-Cu-O 2:2:1:2 has been reported, for instance, by Zhao *et al.*,[10] Lee *et al.*,[11] Huang *et al.*,[12] Ikuta *et al.*,[13] Hasegawa, Nantoh, and Kitazawa,[14] and, using break junctions, by Mandrus *et al.*[15] Completely satisfactory data, especially in the c direction, have been lacking, probably because the extremely short superconducting ξ, especially $\xi_c \sim 1$ Å, makes $G(V)$ extraordinarily sensitive to the *first atomic layer* beneath the barrier, i.e., the BiO layer. This outer layer, exposed by cleavage, is separated from the two central CuO_2 planes, presumed the seat of superconductivity, by $c/2 = 15.4$ Å $\gg \xi_c$. The metallicity of this layer is confirmed, but sensitively depends on stoichiometry, which may locally vary. The superconducting gap Δ_{BiO} in a metallic outer BiO layer may arise by superconducting proximity: A reduced and structure-sensitive gap Δ_{BiO} may be expected. Our measurements presumably sample quasiparticle excitations in the BiO layer with wave vector $\mathbf{k}_c$, because the tunnel barrier is grown on the smooth *ab* plane produced by cleavage. We suspect that this sampling differs from that in the Y-Ba-Cu-O junctions,[8] where many *ab* plane edges were deliberately generated by etching to promote $\mathbf{k}_{ab}$ excitations.

It has been emphasized that clarifying the unusual normal state of the cuprates is an important goal.[16,17] The present work we believe provides some insight into this question. A strength in the use of conventional tunnel junctions, rather than point contact or scanning-tunneling-microscope (STM) methods, is that one can more readily measure the temperature dependence of the spectra. This has enabled us to extract the T dependence of the gap parameter $\Delta(T)$ and of an apparent lifetime energy broadening $\Gamma(T)$. We confirm our earlier report[18] on the importance of pair breaking near T_c, with some quantitative differences, and a more steeply rising $\Gamma(T)$ similar to that of Nicol and Carbotte.[3] The $\Delta(T)$ we now find is non-BCS, with $\Delta(T_c) \approx 0.8\Delta(0)$, and resembles the $\Delta(T)$ predicted by Anderson[17] in an interlayer pairing model. As mentioned earlier, the applicability of Eq. (2) near T_c in the presence of appreciable broadening[3-5] allows us to deduce quantitative values for Δ and Γ in this range, even though the ground-state $N(E)$ function is not accurately known.

We proceed to discuss in turn the experiments, the data and its analysis, to comment on the significance of the results, and to summarize the conclusions.

II. EXPERIMENTAL DETAILS

Conventional tunnel junctions and STM measurements are made on cleaved *ab* planes of large single crystals of 2:2:1:2 grown by directional solidification from a Bi_2O_3-rich melt, following Mitzi *et al.*[19] The crystals are air grown in covered Coors alumina crucibles in a horizontal temperature gradient. Figure 1 shows a prepared junction after masking a center strip with collodion, depositing a cross strip of Pb, and attaching leads with silver paint. The Bi-Sr-Ca-Cu-O material present in millimeter-dimension faces is 2:2:1:2 phase, based on x-ray data [Fig. 2(a)]. The large facets cleave easily with tape. We have no evidence for steps in the faces being studied. As shown in Fig. 2(b), the zero resistance and inductively measured T_c's are typically 90 K. While the ac magnetic susceptibility measured on as-grown material

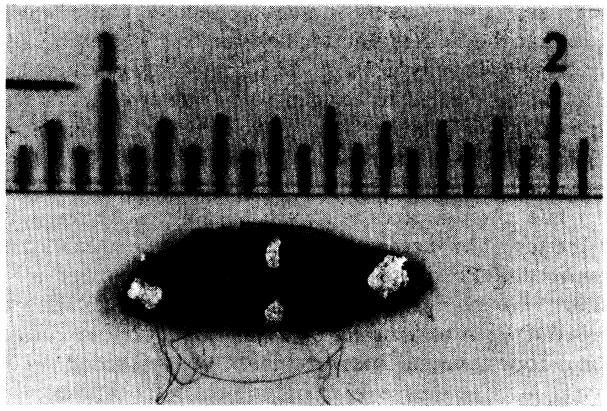

FIG. 1. Tunnel junction formed by masking crystal with collodion, followed by deposit of Pb cross strip and silver paint contacts.

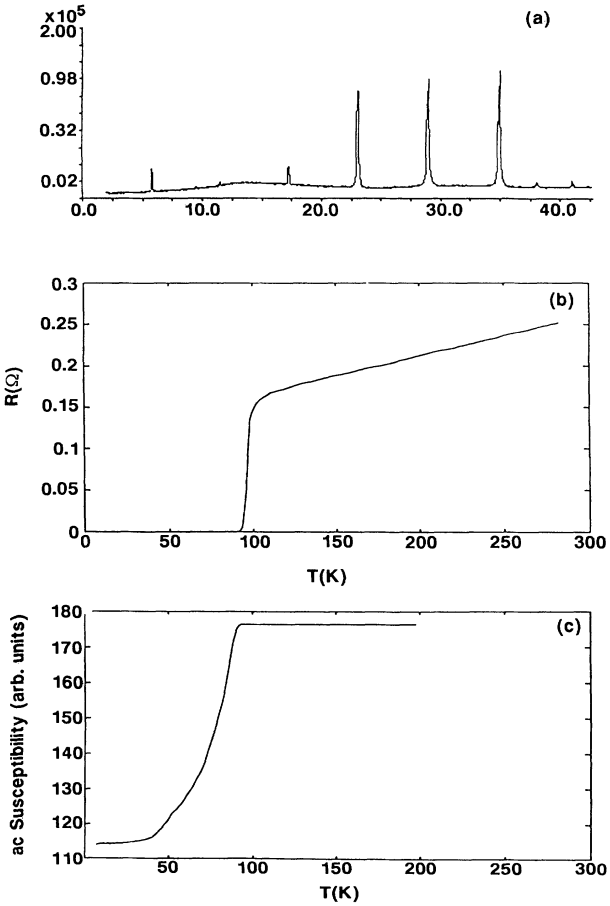

FIG. 2. (a) X-ray diffractometer trace obtained from single-crystal area typical of those on which junctions are formed. Only $(00L)$ diffraction peaks for the 2:2:1:2 phase are present. (b) Resistivity of an as-grown 2:2:1:2 crystal typical of those used in the tunneling study. (c) ac susceptibility measurement on a typical as grown crystal in the tunneling study.

[Fig. 2(c)] may weakly indicate a second phase, we believe that the tunnel junctions on the freely cleaving large facets sample only 2:2:1:2. In some cases crystals have been post-annealed in oxygen to promote a metallic nature of the BiO layer.[20] To make a tunnel junction, the 2:2:1:2 surface is exposed to atmosphere and acquires a native barrier when the counterelectrode, Pb, is deposited. The junction area is about 0.5 mm^2. The resistance of the junction increases with time delay between air exposure and Pb deposit. The form of the barrier is not known, but one possibility is that the Pb reacts with adsorbed oxygen to form an oxide of Pb. dV/dI in conventional four-terminal measurements was recorded on x-y charts at a sequence of temperatures; the curves were later digitized on a 0.5-mV mesh. The same sample holder and thermometer were used in tunneling and resistive and inductive T_c measurements.

The spectroscopic information in $G(V)$ in N-I-S tunneling can be no sharper than 3.5 kT, which can be large, e.g., 23 meV at 77 K. To distinguish the superconducting $G(V)$ variations from the background, we initially fitted to the second derivative $d^2G/dV^2=G''(V)$, which emphasizes the most rapidly varying (superconductivity related) features. The raw data, digitized on 0.5-mV intervals, is initially smoothed by fitting the best least-squares quadratic function on an 8-mV interval about each mesh point. To get $G''(V)$ on a 2-mV mesh, the best quadratic is again fit on an 8-mV range; this time, the coefficient appropriate to $G''(V)$ is evaluated. We confirm that this procedure does not destroy detail in the data.

STM measurements at 4.2 K on the ab cleavage plane were made using a single-tube scanner[21] using Pt-Ir and Nb tips. Crystal and tip were mounted in laboratory air before transfer to the helium Dewar. Revealing data were obtained after the tip deliberately punctured the crystal. As the tip, under servo control, was withdrawn after such a puncture, families of conductance curves $G(V,z)$, only weakly dependent on the vertical displacement z of the tip, were recorded. We suspect that these data arise as electrons tunnel transversely ($\mathbf{k}_{x,y}>\mathbf{0}$) from vertical walls of the tip into ends of the ab planes exposed by the puncture.

III. DATA AND ANALYSIS

The tunneling conductances $G(V,T)$ of more than 20 Pb-I-(Br-Sr-Ca-Cu-O) junctions were investigated. These data are summarized in Fig. 3, where V is the bias of the crystal. All of the junctions in Fig. 3 show strong structure arising from an $N_s(E)$ in the Bi-Sr-Ca-Cu-O electrode. We regard this as an indication that tunneling occurs directly into the superconducting states and strongly samples the nature of these states. In all cases the 4.2-K curves are unlike those of a BCS superconductor with a 26-meV gap: $G(V)=0$, $-26<V<26$ mV and very sharply rising peaks at $V=\Delta=26$ mV. These data reveal $G(0)>0$, with many excitations of energy $E<\Delta$ [even if a constant $G(0)$ is subtracted], and rounded maxima near Δ rather than BCS singularities. The spectra vary somewhat in the sharpness of the superconducting features. Figure 3(a) (junction 2) shows an indication of the Pb gap at $V=0$; Figs. 3(b), 3(c), and 3(d) (junctions 3, 5, and 23, respectively) show smoother, yet still strong, features. The main peak above Δ in $G(V)$ closes and broadens in a non-BCS fashion as T approaches T_c. Outside the gaps occasional sharp structures may relate to the phonons, interlayer interferences,[22] or to junction defects such as microshorts. Figure 3(b) (junction 3) is a bit broader and shows a weak peak or shoulder anomaly inside the main peak which is suggestive of a second gap. However, since this feature remains sharp even near T_c, it may not arise from $N_s(E)$ and may represent a junction defect. The Pb gap feature at $V=0$ is not always seen. This feature is not expected in a Pb-I-S junction where S is a conventional superconductor of gap Δ_s; one rather expects features at $|\Delta_s+\Delta_{Pb}|$ and $|\Delta_s-\Delta_{Pb}|$. If defective portions of the Bi-Sr-Ca-Cu-O surface behave as a normal metal or if Bi-Sr-Ca-Cu-O is truly gapless, the Pb gap will appear at $V=\pm\Delta_{Pb}$, confirming barrier tunneling. In either of the latter cases, the absence of the feature may indicate inelastic processes in the barrier or pair breaking in the surface of the Bi-Sr-Ca-Cu-O electrode, which may distort the $G(V)$ spectrum on the scale $\Delta_{Pb}\cong 1$ meV. Fortunately, this scale is smaller than the 25-meV scale of the features of interest, and we believe $G(V)$ is not seriously affected. Smoothing of the spectra and absence of the Pb feature are characteristic of an aged junction. Still, fitting such data gives a Δ of about 26 meV, similar to that of sharper junctions, indicating that the bias voltage continues to appear across the tunnel barrier. $G(0)$, typically 40% of G at large bias, does not correlate with broadening. The curves of Fig. 3(c) (junction 5) show a smooth $G(V)$ with a strong broad maximum at 30 mV, even at 4.2 K. These data were taken 5 days after junction fabrication. [The Pb gap was observed in $G(V)$ of this junction when it was fresh.]

Since Δ does not coincide with the maximum of $G_s(V)$, the T dependence of Δ cannot be seen intuitively.[18] Fitting via Eq. (1) must be used, which requires [in addition to that of $N_s(E)$ discussed above] choice of $G_n(V)$, ideally corresponding to the same temperature as G_s, to normalize the data.

In the normal state, all junctions in Fig. 3 show a conductance minimum ("pseudogap") at $V=0$, which deepens as T is lowered. Because of the T dependence in the normal state, a serious error might result, e.g., by normalizing a 4.2-K curve with a 90-K curve. This will be correct only if the 90-K curve represents well the state that would result if one could drive the system normal at 4.2 K. Hence, it is important to determine if the T dependence of $G_n(V,T)$, which exists above T_c, also extends to $T<T_c$.

We have taken two approaches to this problem. First, we have found a fitting function for $G_n(V,\ T>T_c)$, which can be extrapolated to lower T, as a possible low-temperature normalization (we find it is not suitable). Second, we analyze each superconducting $G_s(V,T)$ curve individually in a scheme which minimizes dependence on $G_n(V,T)$ and also permits an estimate of the relevant background $G_n(V,T)$. This is done by initially fitting [via Eqs. (1) and (2)] $G''_{Dynes}(V,\Delta,\Gamma,T)$ to $G_s''(V)$, i.e., the cur-

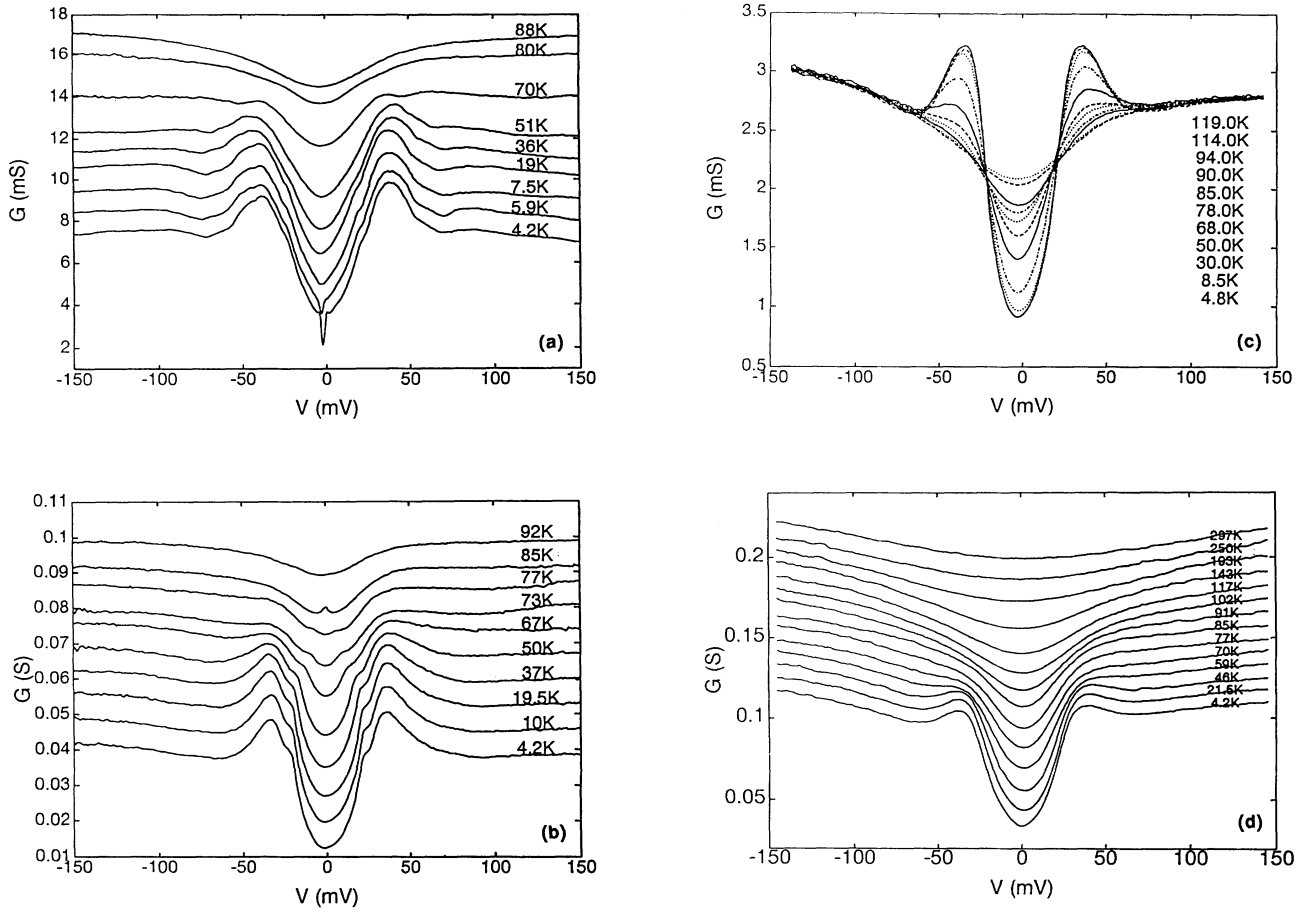

FIG. 3. Survey of tunnel conductance $G(V,T)$ of four Pb-I-(Bi-Sr-Ca-Cu-O) crystal junctions: (a) junction 2, (b) junction 3, (c) junction 5, and (d) junction 23. Calibration in siemens applies to lowest-T curve; others have been successively shifted for clarity.

vature of $G_s(V)$, less sensitive to the broad background $G(V)$ than it is to sharper features in $G_s(V)$. $G(V)$ is then fit to $G_{\text{Dynes}}(V,\Delta,\Gamma,T)+a+bV$, using Δ and Γ chosen above and choosing a,b to fit. The second step in the fitting process gives an estimate of the background, namely, $G_n=1+a+bV$.

We present first (Fig. 4) our fits of $G_n(V,T)$. $G(V)$ above T_c is typically shows a linear region when plotted vs $\ln(V)$. Breaks in this dependence are present in (crystal) positive bias: To minimize this complication we have analyzed $G_n(V)$ for $V<0$. For $V>0$ breaks to smaller slope occur near 67 mV [Fig. 3(a), junction 2], 45 mV [Fig. 3(b), junction 3], 49 mV [Fig. 3(c), junction 5], and 49 mV [Fig. 3(d), junction 23]; this may possibly indicate the top of a band, at 50–70 mV above the Fermi energy in the Bi-Sr-Ca-Cu-O electrode.

In Fig. 5 a logarithmic normal-state background function $G_n=G_b(V,T)$ homogeneous in V and T is compared to $G(V)$ ($V<0$) for junction 5 at $T=119$, 114, and 94 K. The fitting curves are

$$G_b(V)=0.085+0.1\ln[(V^2+(nk_BT)^2]\ ,$$

$n=2.3$. In fits (not shown) to junction 23, the best value of n is 1.9. Mandrus *et al.*[15] report that such a logarithmic function also fits the background conductance in *c*-direction break-junction tunneling in 2:2:1:2. Deviation of 94-K data from $G_b(V,T)$ (solid curve) at $\ln(V)=3.6$ ($V=37$ mV) is attributed to fluctuation superconductivity (see Fig. 8, below). The dashed curve in Fig. 5 (for junction 5) extrapolates $G_b(V)$ to 36 K. We consider

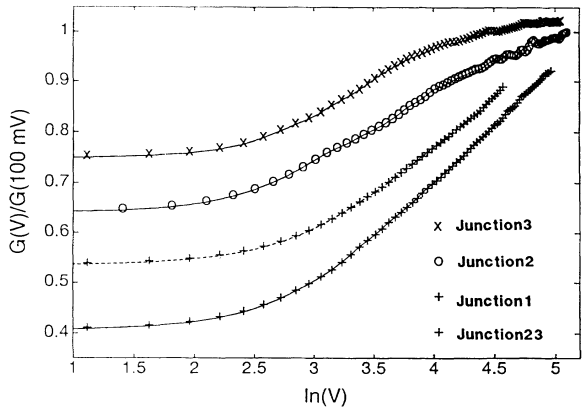

FIG. 4. Summary of $G(V,T_c)$ for junctions 1, 2, 3, and 23 at 93, 88, 92, and 91 K, respectively. Here $G(V)$ values plotted vs $\ln V$ have been normalized by values at 100 mV, and curves for junctions 1 (+), 2 (○), and 23 (+), have been shifted by −0.1, −0.05, and −0.16, respectively.

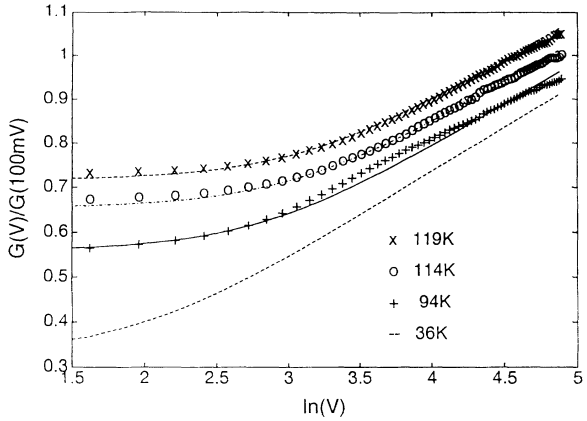

FIG. 5. $G(V)$ (normalized to 100 mV) for junction 5 at 119 K (*), 114 K (○), 94 K (+), plotted vs $\ln(V)$, with V in mV; curves are shifted successively by -0.05 for clarity. Fitting curves are obtained from $G_b(V,T)=0.085+0.1\ln(V^2+\Gamma^2)$, where Γ^2 values for junction 5, 119 K (*), 114 K (○), and 94 K (+), respectively, are 550, 490, and 310 mV^2. Dashed curve is prediction for 36 K; note offset of voltage axis.

below whether or not this extrapolation is physically plausible.

To investigate this question we have followed a second approach, fitting Eqs. (1) and (2) in two steps to individual $G_s(v)$ curves. In the first step we generate $d^2[G_s(V)/G_s(0)]/dV^2$ of the data (i.e., the curvature of the conductance curve) and fit this to $d^2/dV^2[G_{\text{Dynes}}(V,\Delta,\Gamma,T)]$, generated via (1) by choice of Δ and Γ. Note that G'' for $G(V)$ linear or quadratic reduces to a constant, itself small since the curvature of the background (large V) is small compared to curvatures present near $V=0$. In Fig. 6(a), $-0.75G''_{\text{Dynes}}(V, 68\text{ K})$ is shown (+ symbols), compared to the G'' data of junction 5 [Fig. 3(c)] (solid curve, normalized to unity at 100 mV). Dashed and dotted curves are, respectively, $-G''_b(V,T)$ (Fig. 5) evaluated at $T=94$ and 68 K. Calculated points (+) are obtained from Eq. (1) as $-0.75G''_{\text{Dynes}}(V,\Delta,\Gamma,T)$, with $\Delta=21$ meV, $\Gamma=10.5$ meV, scaled by a single constant factor 0.75 to adjust for prior normalization to unity at 100 mV. (This constant is maintained for all curves for junction 5.) The positive swing in $-G''$ at 25 mV

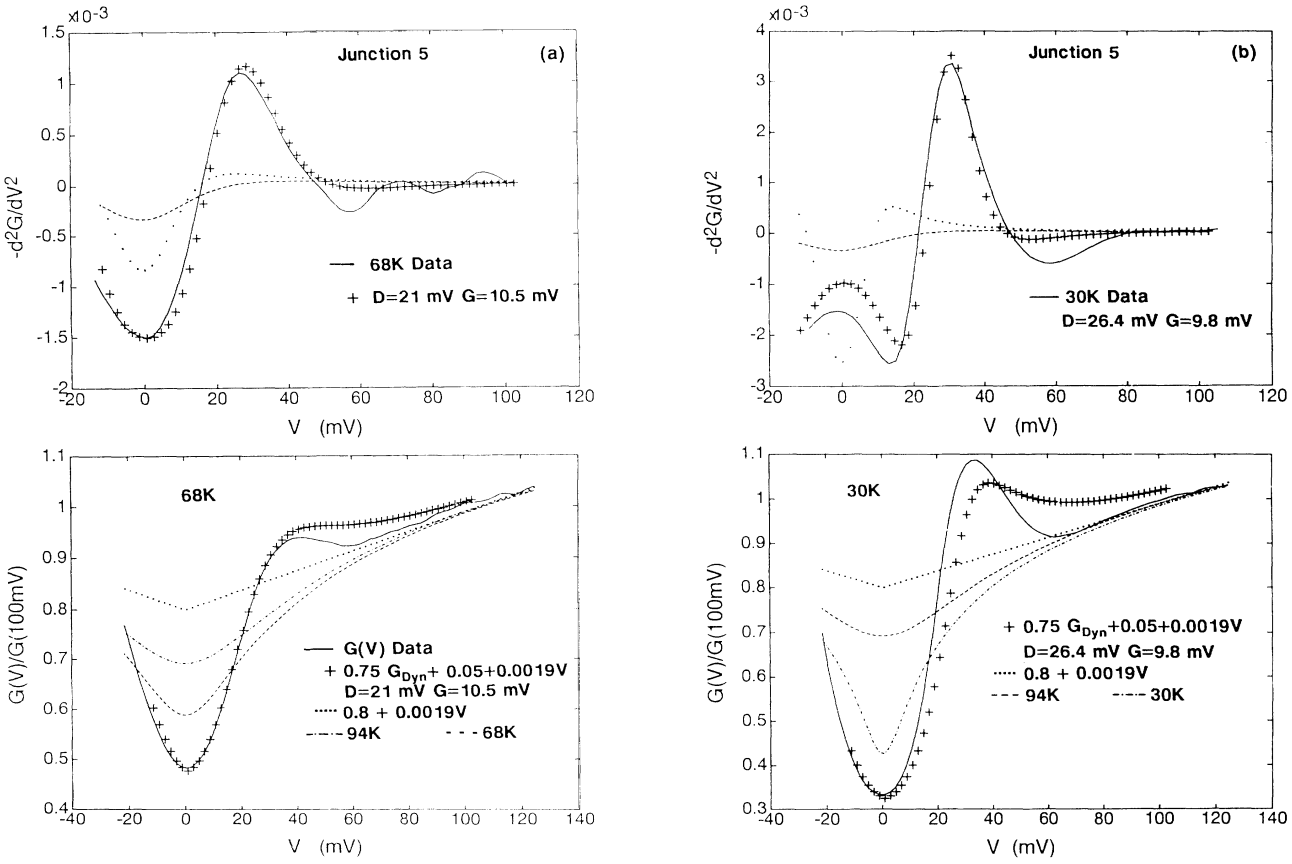

FIG. 6. $G(V)$ and $-G''(V)$ fits to data at high temperatures, assuming lifetime-broadened BCS (Dynes) function in Eq. (1), resulting in $G_{\text{Dynes}}(V,\Delta,\Gamma,T)$ (convolution) with Δ (meV); Γ (meV); T = temperature in K. (a) Upper panel. Solid curve is $-G''(V)$ for junction 5 at 68 K, calculated numerically from $G(V)$ normalized to unity at 100 mV. Dashed and dotted curves are, respectively, $-G''_b(V,T)$ (shown in Fig. 5) evaluated at 94 and 68 K. (a) Lower panel. Application of D,G inferred from $-G''$ fit (in upper panel) to predict conductance $G(V)$. Here shown (+) is $G(V)=0.75G_{\text{Dynes}}(V,\Delta=21\text{ meV},\Gamma=10.5\text{ meV},T=68\text{ K})+0.05+0.0019V$. Dotted curve is the normal state $G(V)$ implied by this fit ($G=0.75+0.05+0.0019V$); dot-dashed and dashed curves are the background conductance $G_b(V,T)$ (see Fig. 5) evaluated at 94 and 68 K, respectively. (b) Upper and lower panels repeat analysis of (a) on data of junction 5 at 30 K. The only parameters changed in the fits are T (measured) and Δ and Γ (adjusted to fit). The previously inferred linear background is unchanged.

occurs in a bias V range where $G_b''(V)$ is quite flat and clearly indicates superconductivity. Success of direct comparison with Eq. (1) [i.e., neglecting any V dependence from the normal state $G(V)$] near $V=0$ suggests that the T dependence of $G_b(V,T)$ does not extend below T_c, but is arrested in the superconducting state.

The second step of the fitting to $G_s(V)$, choice of a constant and linear term, is shown in the lower panel of Fig. 6(a). Here the fit Δ and Γ from G'', and choice of a constant and linear term, fit the $G(V)$ for junction 5 at 68 K. Integrating $-0.75G''_{\text{Dynes}}(V)$ twice to obtain $G(V)$ permits choice of a constant and linear term in V, to fit. The fit shown (+) is

$$G(V)=0.75G_{\text{Dynes}}(V,\ \Delta=21\ \text{meV},\ \Gamma=10.5\ \text{meV},\ T=68\ \text{K})+0.05+0.0019V\ .$$

This function (characteristically) fails to fit accurately just above the mean peak (here near 60 mV), but otherwise the + points well represent $G_s(V)$. Setting $G_{\text{Dynes}}=1$ provides a normal-state curve: the dotted curve is $G_n=0.75+0.05+0.0019|V|$. The dot-dashed and dashed curves are the background conductance $G_n(V,T)$ (see Fig. 5) evaluated at $T=94$ and 68 K, respectively. The fit represented by the + symbols [calculated superconducting $G(V)$] and the dotted line [calculated normal $G(V)$] to the superconducting data (solid curve) carries two assumptions: (1) that the actual $G_s(V)$ for $T\sim T_c$ approximates $G_{\text{Dynes}}(V,\Delta,\Gamma,T)$ and (2) that variations in $G_b(V)$ quadratic or higher order in V can be neglected. Within this framework the fit generates a normal-state conductance (dotted curve), which seems a plausible linearized approximation to the normal-state conductance. The *correct* background conductance is not specified, but may lie intermediate between the linear prediction (dotted) and the dot-dashed line [$G_b(V,T_c)$]. The dashed line representing the extrapolated $G_b(V,68\ \text{K})$ seems implausible.

In Fig. 6(b) the analysis of Fig. 6(a) is repeated on data of junction 5 at 30 K. The only parameters changed in the fits are T (measured) and Δ and Γ (adjusted), leaving the previously inferred linear normal state $G(V)$ unchanged. In upper panel the reasonable modeling of the negative peak $-G''$ at $V=0$, completely at variance with the sharp dip at $V=0$ in the 30-K extrapolated $G_b''(V,T)$ (dots), again suggests that the logarithmic background T dependence is arrested below T_c. The $G_{\text{Dynes}}(V,\Delta,\Gamma,T)$ fit to the details of $G(V)$ beyond the $V=\Delta$ peak in the data is noticeably worse than at 68 K; even so, the essentials of the superconductivity are roughly fit. In the lower panel the discrepancy between the extrapolated $G_b(V,30\ \text{K})$ (dot-dashed curve) in comparison to the data (solid curve), calculated superconducting (+ symbols), and fitted linearized normal state (dotted curve) is quite striking. Considering the data and fits in Fig. 6, it appears that the superconducting features in $G''(V)$ and $G(V)$ are being reasonably approximated at 68 K if not at 30 K, leading one to expect physically meaningful values of $\Delta(T)$ and $\Gamma(T)$ for $T>68$ K. It seems likely that the correct normal state is intermediate between the linearized function resulting from the fits (dotted curve, in lower panels) and $G_b(V,T_c)$, and that the background obtained by extrapolating $G_b(V,T)$ at low temperature is irrelevant.

As a further test, we predict $G(0,T)$, using Δ,Γ fitted as above. In Fig. 7 plots of $G(0,T)/G(100\ \text{mV},T)$ for junctions 5 (○) and 23 (+) show weak discontinuities of slope at junction T_c's estimated as 90 and 87 K, respectively, close to crystal T_c of 90 K. As emphasized in Ref. 7, where similar results were obtained on Y-Ba-Cu-O, a *junction* discontinuity at the *crystal* T_c indicates that tunneling probes intrinsic superconducting properties of the Bi-Sr-Ca-Cu-O. The solid curve in Fig. 7 is

$$1.86G_b(V,T)=-0.1+0.12\ln[V^2+(1.9k_BT)^2]\ ,$$

evaluated at $V=0$. The factor 1.86 renormalizes to $G=1$ at $V=0$, $T_c=87$ K, from $V=100$ mV. The parameters of $G_b(0,T)$ come from $G_b(V,T)$ vs $\ln(V)$ plots for junction 23 (not shown, similar to those of Fig. 5). For $T<T_c$, $G(0,T)$ data [junction 23 (+), junction 5 (○)] are fit with curves [junction 23 (dashed curve), junction 5 (dot-dashed curve)] calculated from Eq. (1) using

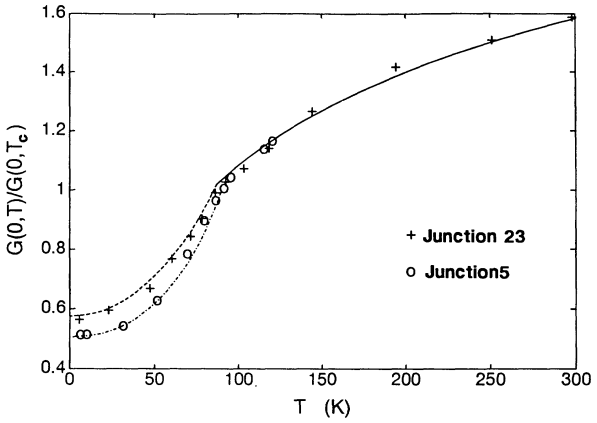

FIG. 7. Normalized zero-bias conductances $G(0,T)$ for junctions 5 (○) and 23 (+) show weak discontinuities at junction T_c's, estimated as 90 and 87 K, respectively, which are close to crystal T_c of 90 K. Solid curve is obtained from fit to high-temperature background conductance for junction 23; the low-temperature dashed and dot-dashed curves are obtained from $G_{\text{Dynes}}(0,\Delta(T),\Gamma(T),T)$ (see text).

$G_{\text{Dynes}}(0,\Delta,\Gamma,T)$ normalized to unity at T_c. *This fitting procedure assumes that* $G_n(0,T)$ *is constant below* T_c. Since the extrapolated $G_b(0,T)$ falls rather sharply between 87 and 4.2 K, the success of the fit in Fig. 7 for $T<T_c$ is evidence in that the $\ln(T)$ dependence of $G_b(0,T)$ is arrested at T_c. [The fits assume $\Delta(T)$ and $\Gamma(T)$ similar but not identical to those shown in Fig. 9 below.]

The points in Fig. 7 just above T_c may lie slightly below the solid curve representing $G_b(0,T)$, although the precision of the data and fit do not allow a definite conclusion. Such an effect is expected, as occurs in the resistivity $\rho(T)$ and arising from superconducting fluctuations.

Figure 8 provides spectroscopic evidence for fluctuation superconductivity above T_c in $-d^2G/dV^2$ of junction 5 at $T=94$ and 90 K. At each temperature the dots represent

$$-\frac{d^2}{dV^2}\ln[V^2+(2.3k_BT)^2]=-G_b''(V)$$

(see Fig. 4). Within error, it appears that the background accounts for the data at $T=119$ and 114 K. At $T=94$ and $T=90$ K, however, an overshoot is seen. The + and * symbols plot $-0.75G''_{\text{Dynes}}(V,$ 21 meV, 25 MeV, 94 K) and $-0.75G''_{\text{Dynes}}(V,$ 19.2 meV, 20 meV, 90 K), respectively. Since the peak near 35 mV appears in a range where $-G_b''(V)$ is quite flat, it is regarded as a signal of superconductivity.

Figure 9 summarized the T dependence of the fitted $\Delta(T)$ and $\Gamma(T)$ for junctions 5 and 23 (see Figs. 6 and 8). Although the fit values are shown even for low temperatures, we emphasize that the parameter values are expected to be physically meaningful for high temperatures where Eq. (2) is justified. $\Delta(T)$ for junctions 5 (○) and 23 (+) (connected by an arbitrary smooth curve) is strongly non-BCS in that it falls by only about 25% at T_c. The $\Delta(T)$ values for junction 5 above T_c, at $T=90$ and 94 K, are attributed to fluctuations, as mentioned above. T_c occurs near the crossing of $\Delta(T)$ and $2.3k_BT$ (dot-dashed), the $T>T_c$ broadening inferred from $G_b(V,T)$. The inferred $G(T)$ for junction 5 (+) rises sharply to about $2.3k_BT$ at T_c. The dashed line is $\Gamma(T)=10+8200\exp(-2\Delta_0/k_BT)$ meV. Here $\Delta_0=\Delta(0)=26$ meV. This might suggest that lifetime broadening occurs as ("preexisting") pairs with full $T=0$ binding energy thermally break up and recombine. The origin of the $T=0$ *limit* of the broadening, $\Gamma\sim10$ meV, is unclear and represents to some extent the inadequacy of Eq. (2) to describe the ground state. This could result

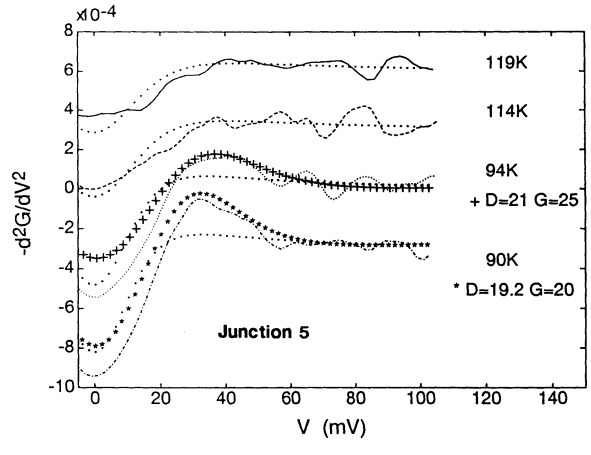

FIG. 8. $-d^2G/dV^2$ spectra of junction 5 in range 119–90 K, above crystal T_c, show evidence of fluctuation superconductivity at 94 and 90 K. At each temperature widely spaced dots are $-G_b''(V)$, second derivative of background conductance (see Fig. 4). The + and * symbols plot $-0.75G''_{\text{Dynes}}(V,$ 21 meV, 25 meV, 94 K) and $-0.75G''_{\text{Dynes}}(V,$ 19.2 meV, 20 meV, 90 K), respectively. The 94-K trace is unshifted; others are shifted for clarity in units of 3×10^{-4}.

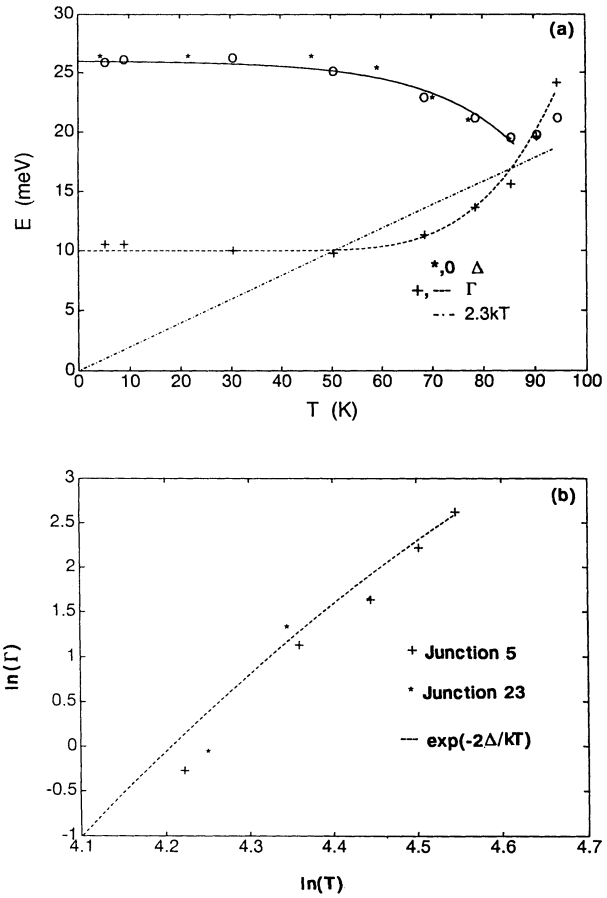

FIG. 9. (a) T dependence of gap (Δ) and broadening (Γ) from fits (see text) for junctions 5 and 23, Δ for junction 5 (○), and junction 23 (+) are connected by an arbitrary smooth curve. The Δ values for junction 5 at $T=90$ K are attributed to fluctuation superconductivity. The dot-dashed line plots $2.3k_BT$; inferred Γ for junction 5 (+) is compared with the dashed line representing $G=10+8200\exp(-2\Delta_0/k_BT)$ meV, with $\Delta_0=26$ meV. All fits represented in this plot have properly accounted for thermal broadening via Eq. (1). (b) Broadening vs temperature, with constant low-temperature broadening subtracted. The dashed line is $8200\exp(-2\Delta_0/k_BT)$, with $\Delta_0=26$ meV, shown in (a). The + symbols represent G(junction 5)-10 meV; the * symbols are G(junction 23)-12 meV.

in fits to Eq. (2) if the true spectrum were rounded, e.g., as predicted by Mila and Abrahams.[23] However, some variability of the $T=0$ limit of Γ in our data suggests an extrinsic contribution, possibly from barrier imperfection. The high-temperature values and sharply rising T dependence of Γ are similar in all junctions and are believed to be intrinsic.

In Fig. 10 we consider the normalized ground-state DOS. The fits presented in Fig. 6, which indicate that the normal-state minimum ("pseudogap") does not deepen for $T<T_c$, can justify $G(V,T_c)$ for normalization. In Fig. 10(a) the 4.2-K curve for junction 5 is presented as normalized by the 94-K curve. Here $G(0)$ is 0.45, and there would be many states in the gap (i.e., at arbitrarily low excitation energy) even if $G(0)=0.45$ were subtracted as an artifact. The positive peak is broader, yet cuts off more sharply than BCS, with some suggestion of a negative swing in $G(V)$ in the range 60–80 meV above the main peak. There is no chance of describing this spectrum using the lifetime-broadened BCS model represented by Eq. (2). The rounded shape at low V and $G(0)$ up to 0.2 or so can be explained if the gap function itself is zero on a point or line of points on the Fermi surface.

Klemm and Liu[24] have studied superconductivity produced by interlayer pairing in models of layered metallic structures. Their models allow hopping and pairing of carriers between adjacent metallic planes, up to $N=4$ layers per unit cell, Fig. 10(b) is $N_s(E)$ calculated by Liu and Klemm[24] for Bi-Sr-Ca-Cu-O, modeled as two CuO_2 planes and one BiO plane per unit cell. Gaplessness (V shape) arises from a node of Δ_c, a consequence of interlayer pairing. The small $G(0)=0.2$ shown here comes from numerical smearing of the V-shaped DOS. The split gap shown in this figure, which may describe an inner gap feature of the $G(V)$ reported for Y-Ba-Cu-O,[8] is not clearly present in our data, although it is suggested in Fig. 3(b). Slightly different parameters in the model[24] might merge the gaps leaving the V shape and $G(0)=0.2$. The model of Ref. 22 apparently allows much larger $G(0)>0$: at the moment we are unclear on the discrepancy on this point with the apparently more complete calculation leading to Fig. 10(b).

If the $G(0)>0$ in our data is an artifact, it may be appropriate to study $G(V)-G(0)$, as shown in Fig. 10(c) for the 4.2-K curve of junction 5, normalized by $G(V$, 94

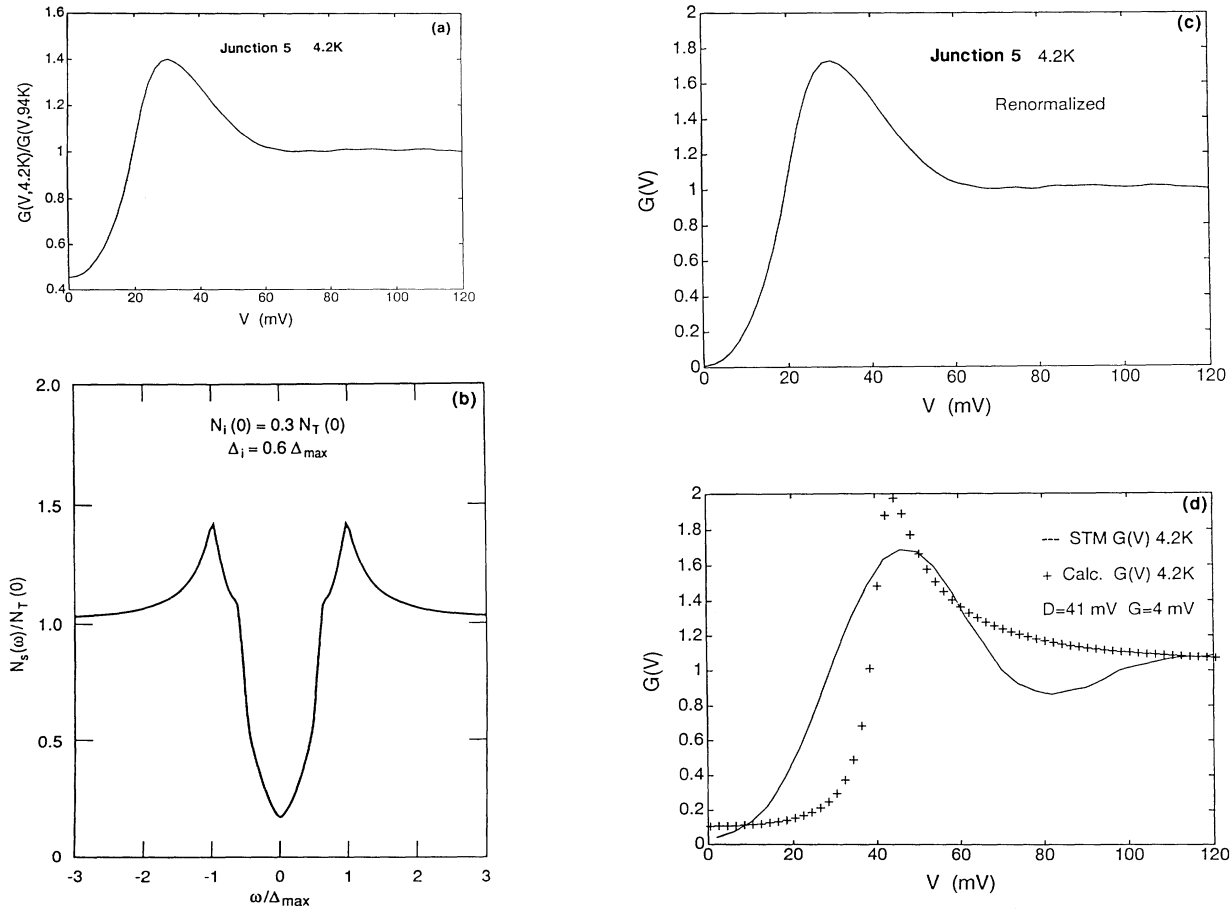

FIG. 10. (a) Normalized conductance $G(V,T)/G(V,94\text{ K})$ for junction 5. (b) Gapless $G(V)$ predicted by Liu and Klemm on layering model for Bi-Sr-Ca-Cu-O (Ref. 24). (Figure reproduced with permission from author of Ref. 24.) (c) Normalized conductance $G(V,T)/G(V,94\text{ K})$ for junction 5 with $G(0)$ subtracted. This curve cannot be fit by BCS including lifetime broadening. (d) $G(V)$ for STM junction to Bi-Sr-Ca-Cu-O, believed to more closely sample the CuO_2 planes.

K). This renormalized curve cannot be fit by Eq. (2), as the positive peak is larger and broader yet cuts off more sharply at higher V. The rounded shape at $V=0$ in $G(V)-G(0)$ will not result from Eq. (2), but might be explained along lines presented in Refs. 23 or 24 or in other ways.

In Fig. 10(d) is shown a $G(V)$ for a STM junction on Bi-Sr-Ca-Cu-O at 4.2 K, which shows $G(0)$ nearly zero, but indicates low-energy excitations ("states in the gap") with a rapidly rising low-energy conductance. The pronounced dip at 80 mV resembles that observed in photoemission.[25] The Δ for this spectrum must be significantly larger, as suggested by comparison with $G_{\text{Dynes}}(V, 41$ meV, 4 meV, 4.2 K) (+ symbols). Clearly, the lifetime-broadened BCS model does not fit, but may correctly indicate that Δ is larger in the STM spectrum of Fig. 10. It is possible that this spectrum is associated more directly with the CuO_2 planes than with the BiO surface sampled by most of our data.

IV. DISCUSSION

A. Normal state

In the normal state just above T_c, we find a weak minimum or "pseudogap" centered at $V=0$, which can be approximated as $G(V,T)=\alpha \ln[(eV)^2+(nk_BT)^2]$, where k_B is Boltzmann's constant and n is near 2, in agreement with the results of Mandrus *et al.*[15], also for c-direction tunneling. The idea of a short lifetime in the normal state, $\Gamma=\hbar/\tau\approx 2k_BT$, seems well established in theory and experiment for the cuprates.[3] The $G(V)$ minimum noticeably deepens as T is reduced; such behavior is characteristic of tunneling into a system of localizing states. A weak logarithmic singularity in V, cut off by $2k_BT$ at small bias, is plausible for tunneling along the c direction where localization is signaled by the rising resistivity as T approaches T_c. The question of whether this T dependence extends below T_c is important, as we have mentioned above, in connection with normalizing the $G(V,T)$ curves to compare with theory via (1). Our results suggest that c-direction localization is arrested at T_c, as assumed in the fits in Fig. 6 and in modeling the T dependence of $G(0)$ in Fig. 7. This conclusion on c-direction transport seems consistent with the idea of dimensional crossover from two dimensions (2D) to 3D below T_c in the interlayer pairing theory.[16,17] In contrast, the $G_n(V)$ expected for tunneling into $\mathbf{k}_{x,y}$ states in the ab plane is apparently of the form $A+B|V|$ (apart from weak effects of the tunneling barrier) observed in etched Y-Ba-Cu-O-Pb junctions.[8] We suspect that ab-direction tunneling may be relatively important in the Y-Ba-Cu-O study,[8] consistent with etch pits exposing ab-plane terminations resulting from the chosen junction fabrication. In the ab-direction break-junction study of 2:2:1:2 by Mandrus *et al.*,[15] however, the background $G(V)$ was not linear, as one would expect, but decreased at high bias, somewhat as earlier reported in high-current-density point contacts.[12] The recent STM study of Hasegawa, Nantoh, and Kitazawa[14] finds that the background conductance differs with tip height above the ab plane (barrier transmission), as if different sets of states may be sampled at different distances; possibly, d states become more important with thin barriers. The consequences of high current density such as local heating or nonequilibrium may also play a role in affecting the $G(V)$ at high bias.

In the present case, having recognized the normal state "pseudogap" characteristic of the c direction, confirming Ref. 15, it appears that the c-direction states are sampled.

B. $\Delta(T)$ and $\Gamma(T)$ near T_c

As discussed earlier, we expect that analysis of the $G(V)$ data near T_c making use of Eqs. (1) and (2) leads to quantitatively useful values of $\Delta(T)$ and $\Gamma(T)$ even though Eq. (2) does not a describe the ground state. Fitting initially to $G''(V)$ appears to minimize problems due to background and the nonzero $G(0)$, much as in the work of Leger *et al.*[26] where this technique was first used. We also confirm our earlier finding, using a simplified analysis neglecting the thermal convolution,[18] of a broadening $\Gamma(T)$ rapidly rising near T_c. We find at T_c a large $\Delta(T_c)\approx 0.8\Delta(0)\approx nk_BT_c$ with n about 2 and that the values of Δ and Γ are nearly equal. The factor n (1.9 in junction 23, 2.3 in junction 5) may be high, since Eq. (1) has not been applied to the DOS underlying the pseudogap [contrary to our correct treatment of the superconducting $\Gamma(T)$]. Thus, at T_c, the broadening $\Gamma(T)$ inferred from below roughly matches the high-temperature broadening (cutoff of the log singularity) inferred from fitting $G(V,T)$ above to T_c to $\ln[(eV)^2+nk_BT)^2]$. Our results agree with experimental studies of fluctuations in Y-Ba-Cu-O which provide estimates of pair breaking and transport rates, both near $\hbar/\tau=1.35k_BT$ (Refs. 27 and 28) and governed by inelastic processes, in accordance with the picture presented by Lee and Read.[29] In this picture the large ratio $2\Delta/k_BT_c$ comes from reduction of T_c below T_{c0} by pair breaking: in Ref. 28 it is estimated that T_{c0} in the absence of pair breaking would be 210 K. As a consequence of the more thorough analysis we have carried out here compared with Ref. 18, it now appears that $\Gamma(T)$ as shown in Figs. 9(a) and 9(b) rises more rapidly than the T^3 power previously suggested,[18,30] in fact rather similarly to the $\Gamma(T)$ recently given by Nicol and Carbotte.[3]

We suggest that our gap values may be reasonable estimates for the BiO-vacuum interface at $T=0$, although obtained from fits to higher-temperature data. In Fig. 9(a) one sees that the T variation of Δ occurs mostly in the high-temperature region where our approximate analysis is most valid; so that the low-temperature values are reasonably evident. One sees in Fig. 9(a) that $\Delta(T)$ anomalously remains substantial near T_c. Similar behavior has been inferred from other experiments[7,31–34] and has also been predicted.[17] However, we emphasize that the experimental signature, fitted to infer $\Delta(T),\Gamma(T)$ [i.e., a conductance $G(V)$ of the form of Eqs. (1) and (2)] *disappears* at T_c (see Figs. 6 and 8) except for a fluctuation range of 5–10 K. The functional form of $\Gamma(T)$ shown in

Fig. 9(b) in comparison with $\Gamma(T)$-$\Gamma(0)$ may suggest that pairs of essentially full binding energy are present near T_c. However, the structure remaining in $G(V)$ well above T_c is distinct and associated with normal-state localization, so that if pairs exist well above T_c, they behave independently and do not influence the tunneling $G(V)$.

Substantial agreement exists between our BiO-plane energy-gap estimate 26 meV, obtained from the fitting process described on many samples, with values indicated by several tunneling reports[11,12,15] and with the in-plane gap inferred from high-resolution photoemission spectroscopy.[20,25] However, our value for Δ at the BiO surface is smaller than that indicated in the recent STM study of Hasegawa, Nantoh, and Kitazawa[14] and significantly larger than found in Ref. 33, although the T dependence is similar.

C. Ground-state DOS

The data always indicate a zero-bias conductance $G_s(0)/G_n = 0.4-0.5$, dependent somewhat on the choice of normalization. This is consistent with the observation of the Pb gap feature at $V=0$, although that feature could appear with $G(0)=0$ and with a V-shaped DOS at $V=0$. However, $G(0)>0$ conflicts with two recent reports[14,15] and with our own STM spectrum shown in Fig. 10(d). It is possible that $G(0)=0$ occurs only under particular circumstances, e.g., when the BiO surface locally is nonmetallic or perhaps when and/or where it is metallic a gap function node, as suggested in the Liu-Klemm analysis,[24] appears. However, an interpretation implying intrinsic gaplessness, even if limited to stoichiometry with fully metallic BiO planes, may be difficult to reconcile with measurements of penetration depth and specific heat.[9] We cannot in our results rule out that $G(0)>0$ in the wide-area junctions may arise in part from defective areas which are not superconducting, as has been suggested,[35,36] or even that the effect comes from an imperfect barrier. If we adopt this view and subtract $G(0)$ from the conductance, the resulting curves are still "gapless"; i.e., the shape of the minimum in $G(V)$ at low temperature is more rounded than expected for a BCS superconductor of such a large gap. Low-energy excitations would still remain, proportional to E or E^2. This second aspect of gaplessness exhibited by the data can arise from a gap function with a node at a particular point or line on the Fermi surface. Such an effect occurs even with s-wave pairing of carriers between layers in the model of Klemm and Liu.[24] A different origin of such an effect is repulsive pairing,[17,23] as described by Mila and Abrahams.[23]

The observed $G(V)$ at 4.2 K clearly differs from the BCS form, even if $G(0)>0$ is subtracted and lifetime broadening is included. Lack of an obvious $N_s(E)$ function for fitting $G(V)$ via Eq. (1) is a problem for analyzing the low-temperature data.

Finally, in brief comparison with STM data on the same crystals, under conditions where we suspect electrons tunnel laterally with $\mathbf{k}_{x,y}$ from the tip wall into ab-plane terminations, we see a larger gap, about 40 meV, $G(0)\approx 0$, and a pronounced dip in $G(V)$ at 80 meV. The larger gap is plausibly to be associated with the CuO_2 planes, rather than the BiO planes presumably sampled in the Pb-I-(Bi-Sr-Ca-Cu-O) junctions. The dip feature is seen in photoemission and has been explained by Anderson[16,17] as a consequence of the 2D-to-3D crossover below T_c in his interlayer tunneling mechanism for cuprate superconductivity. At this point we are unable to test the anisotropy of the 80-meV dip that the crossover picture and photoemission imply.

D. What is being sampled below T_c

A large gap is seen in predominantly c-direction tunneling, comparable with that inferred in the ab directions,[15,25] suggesting that the gap function in 2:2:1:2 is roughly isotropic. Kirtley[37] has shown that very small barrier heights, unlikely for a grown barrier, would be needed to strongly sample $\mathbf{k}_{x,y}$ with our geometry. Our observation of a large gap along $\mathbf{k}_c$ may support the idea of dimensional crossover to 3D below T_c mentioned above, which predicts a $\Delta(k)$ which is not a strong function of direction $\mathbf{k}$.[17] An *isotropic* gap is also predicted in the interlayer model[24] for Bi-Sr-Ca-Cu-O treated with $N=2$ metallic planes/unit cell. One intuitively expects the spatial variation of Δ in the BiO-CuO_2-BiO sandwich, of width 15.4 Å $\gg \xi_c$, to tend to lower Δ on the outer surfaces relative to the central CuO_2 planes where superconductivity is presumably generated. Tentative evidence for a larger gap in the CuO_2 plane is presented here in Fig. 10(d). The depression of Δ at the BiO planes would, if similar to the proximity effect in conventional systems, depend very sensitively, given the extremely short coherence length ξ_c, on the carrier scattering length l, which will be related to the stoichiometry and level of defects present. Hence one may expect the observability and magnitude of the gap in the BiO plane to be very sensitive to sample preparation, as is well known in tunneling and photoemission experiments. Alternatively, from the viewpoint of the interlayer models,[24] variation in the stoichiometry, and hence metallicity of the BiO planes and appropriate N in the model, should lead to characteristically different and predictable conductance spectra.

V. CONCLUSIONS

We believe that our results have a bearing on basic issues relating to superconductivity of the cuprates. However, our conclusions depend to some extent on two assumptions. First, the junctions are imperfect, exhibiting some extraneous broadening. We believe this is limited to the scale of a few millivolts, small on the scale of the features of interest. We cannot entirely rule out other distortions from the junction imperfections. Second, for lack of a better fitting function, the data have been analyzed using a lifetime-broadened BCS density of states [Eq. (2)]. As we have indicated, this can be strictly justified only near T_c in systems with large level broadening. In our opinion, Bi-Sr-Ca-Cu-O is such a system. With these assumptions the data analyzed near T_c sup-

port a non-BCS picture of the superconducting transition occurring when a pair-breaking rate $\Gamma(T)=\hbar/\tau_\phi$ rises to match $\Delta(T_c)\approx 0.8\Delta(0)\approx\hbar/\tau_t$, with τ_t for transport and τ_Φ for pair breaking reflecting an inelastic process. The temperature dependence and apparent approximate isotropy of $\Delta(T)$, and the inferred arrest of c-direction localization below T_c, seem consistent with the interlayer tunneling mechanism of superconductivity proposed by Anderson.[17]

ACKNOWLEDGMENTS

We have benefited from discussion with R. A. Klemm and S. H. Liu and gratefully acknowledge the use of Fig. 10(b) from S. H. Liu. We acknowledge discussion and valuable assistance from Zhao Y. Rong and D. B. Mitzi regarding crystal growth. The work was supported by U.S. Department of Energy, Office of Basic Energy Sciences under Grant No. DE-EG02-87ER45301.

*Permanent address: Institute of Physics, Chinese Academy of Sciences, Beijing, China.

[1]W. L. McMillan and J. M. Rowell, in *Superconductivity,* edited by R. D. Parks, (Dekker, New York, 1969), Vol. 1, p. 561.

[2]See E. L. Wolf, *Principles of Electron Tunneling Spectroscopy* (Oxford University Press, New York, 1989).

[3]E. J. Nicol and J. P. Carbotte, Phys. Rev. B **44**, 7741 (1991) (see Fig. 3).

[4]R. C. Dynes, V. Narayanamurti, and J. P. Garno, Phys. Rev. Lett. **41**, 1509 (1978); for application to spin fluctuations, see T. Koyama and M. Tachiki, Phys. Rev. B **39**, 2279 (1989).

[5]P. G. de Gennes, *Superconductivity of Metals and Alloys* (Benjamin, New York, 1966); see also R. W. Cohen, B. Abeles, and C. R. Fuselier, Phys. Rev. Lett. **23**, 377 (1969).

[6]Q. Huang, J. F. Zasadzinski, N. Tralshawala, K. E. Gray, D. G. Hinks, J. L. Peng, and R. L. Greene, Nature **347**, 369 (1990).

[7]J. Geerk, X. X. Xi, and G. Linker, Z. Phys. B **73**, 329 (1988).

[8]M. Gurvitch, J. M. Valles, Jr., A. M. Cucolo, R. C. Dynes, J. P. Garno, L. F. Schneemeyer, and J. V. Waszczak, Phys. Rev. Lett. **63**, 1008 (1989); J. M. Valles *et al.*, Phys. Rev. B **44**, 11 986 (1991).

[9]B. Battlogg, in *High Temperature Superconductivity Proceedings,* edited by K. S. Bedell, D. Coffey, D. E. Meltzer, D. Pines, J. R. Schrieffer (Addison-Wesley, Reading, MA, 1990); Phys. Today **44**(6), 44 (1991).

[10]S. P. Zhao, H. J. Tao, Y. F. Chen, Y. F. Yan, and Q. S. Yang, Solid State Commun. **67**, 1179 (1988).

[11]M. Lee, D. B. Mitzi, A. Kapitulnik, and M. R. Beasley, Phys. Rev. B **39**, 801 (1989).

[12]Q. Huang, J. F. Zasadzinski, K. E. Gray, J. Z. Liu, and H. Claus, Phys. Rev. B **40**, 9366 (1989).

[13]H. Ikuta, A. Maeda, K. Uchinokura, and S. Tanaka, Jpn. J. Appl. Phys. **27**, L1038 (1988).

[14]T. Hasegawa, M. Nantoh, and K. Kitazawa, Jpn. J. Appl. Phys. **30**, L276 (1991).

[15]D. Mandrus, L. Forro, D. Koller, and L. Mihaly, Nature **351**, 460 (1991).

[16]P. W. Anderson, Phys. Rev. B **42**, 2073 (1990); Phys. Rev. Lett. **67**, 660 (1991); in Ref. 9, and references therein.

[17]P. W. Anderson (unpublished).

[18]E. L. Wolf, H. J. Tao, and B. Susla, Solid State Commun. **77**, 519 (1991).

[19]D. B. Mitzi, L. W. Lombardo, A. Kapitulnik, S. S. Laderman, and R. D. Jacowitz, Phys. Rev. B **41**, 6564 (1990).

[20]B. O. Wells, Z. X. Shen, D. S. Dessau, W. E. Spicer, C. G. Olson, D. B. Mitzi, A. Kapitulnik, R. S. List, and A. Arko, Phys. Rev. Lett. **65**, 3056 (1990).

[21]A. P. Fein, J. R. Kirtley, and R. M. Feenstra, Rev. Sci. Instrum. **58**, 1806 (1987).

[22]M. Tachiki, S. Takahashi, F. Steglich, and H. Adrian, Z. Phys. B **80**, 161 (1990).

[23]Frederic Mila and E. Abrahams, Phys. Rev. Lett. **67**, 2379 (1991).

[24]R. A. Klemm and S. H. Liu, Physica C **176**, 189 (1991); S. H. Liu and R. A. Klemm, Chin. J. Phys. (Taipei) **29**, 157 (1991); R.A. Klemm and S. H. Liu, Phys. Rev. B **44**, 7526 (1991); S. H. Liu and R. A. Klemm, *ibid.* **45**, 415 (1992).

[25]D. S. Dessau, B. O. Wells, Z. X. Shen, W. E. Spicer, A. J. Arko, R. S. List, D. B. Mitzi, and A. Kapitulnik, Phys. Rev. Lett. **66**, 2160 (1991).

[26]A. Leger, J. Klein, M. Belin, and D. Defourneau, Solid State Commun. **11**, 1331 (1972).

[27]A. G. Aronov, S. Hikami, and A. I. Larkin, Phys. Rev. Lett. **62**, 965 (1989).

[28]K. Semba, T. Ishii, and A. Matsuda, Phys. Rev. Lett. **67**, 769 (1991). See also discussion of B. Batlogg in Ref. 9.

[29]P. A. Lee and N. Read, Phys. Rev. Lett. **58**, 2629 (1987).

[30]L. Coffey, Phys. Rev. Lett. **64**, 1071 (1990).

[31]Z. Schlesinger, R. T. Collins, F. Holtzberg, C. Feild, G. Koren, and A. Gupta, Phys. Rev. B **41**, 11 237 (1990).

[32]J. E. Demuth, B. N. J. Persson, F. Holtzberg, and C. V. Chandrasekhar, Phys. Rev. Lett. **64**, 603 (1990); B. N. J. Persson and J. E. Demuth, Phys. Rev. B **42**, 8057 (1990).

[33]L. C. Brunel, S. G. Louie, G. Martinez, S. Labdi, and H. Raffy, Phys. Rev. Lett. **66**, 1346 (1991).

[34]D. van der Marel, M. Bauer, E. H. Brandt, H. U. Habermeier, D. Heitmann, W. Konig, and A. Wittlin, Phys. Rev. B **43**, 8606 (1991).

[35]T. Komeda, G. D. Waddill, P. J. Benning, and J. H. Weaver, Phys. Rev. B **43**, 8713 (1991); see also Ref. 32.

[36]J. C. Phillips, Phys. Rev. B **41**, 8968 (1990).

[37]J. R. Kirtley, Phys. Rev. B **41**, 7201 (1990).

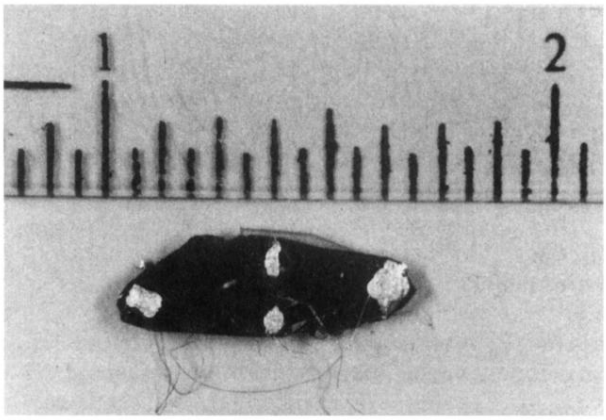

FIG. 1. Tunnel junction formed by masking crystal with collodion, followed by deposit of Pb cross strip and silver paint contacts.